GAS MEDIATED CHARGED PARTICLE BEAM PROCESSING OF NANOSTRUCTURED MATERIALS

C.J.Lobo[1], A.A. Martin[1], C. Elbadawi[1], J. Bishop[1], I. Aharanovich[1] & M.Toth[1*]
[1] School of Physics and Advanced Materials, University of Technology Sydney, NSW Australia
[*]Corresponding author email: milos.toth@uts.edu.au

Abstract

Gas mediated processing under a charged particle (electron or ion) beam enables direct-write, high resolution surface functionalization, chemical dry etching and chemical vapor deposition of a wide range of materials including catalytic metals, optoelectronic grade semiconductors and oxides. Here we highlight three recent developments of particular interest to the optical materials and nanofabrication communities: fabrication of self-supporting, three dimensional, fluorescent diamond nanostructures, electron beam induced deposition (EBID) of high purity materials via activated chemisorption, and post-growth purification of nanocrystalline EBID-grown platinum suitable for catalysis applications.

Keywords: electron beam induced processing, nanofabrication, etching, deposition, charged particle beam processing, surface functionalization

1. INTRODUCTION

Gas-mediated ion and electron beam processing [1] enable direct-write, additive and subtractive lithography without the use of stencils or lithographic masks (Fig. 1). The geometry of interest is realized either by scanning a tightly focused beam over a substrate, or by using a shaped beam with a specific flux profile. Common applications include the fabrication of nanodot and wire arrays [2], magnetic nanowires [3] and tips for magnetic force microscopy [4]. It has also been used to make electrical contacts to carbon nanotubes [5] and to fabricate plasmonic nanostructures [6] and metallic seeds that localize and catalyze the growth of nanowires [7]. Recently, gas-mediated electron beam processing has been applied to surface functionalization, and used to write chemically active surface regions that promote room temperature chemical vapor deposition [8-13], molecular exchange reactions with single-stranded DNA [14], and chemical dry etching of ultra nanocrystalline diamond [15].

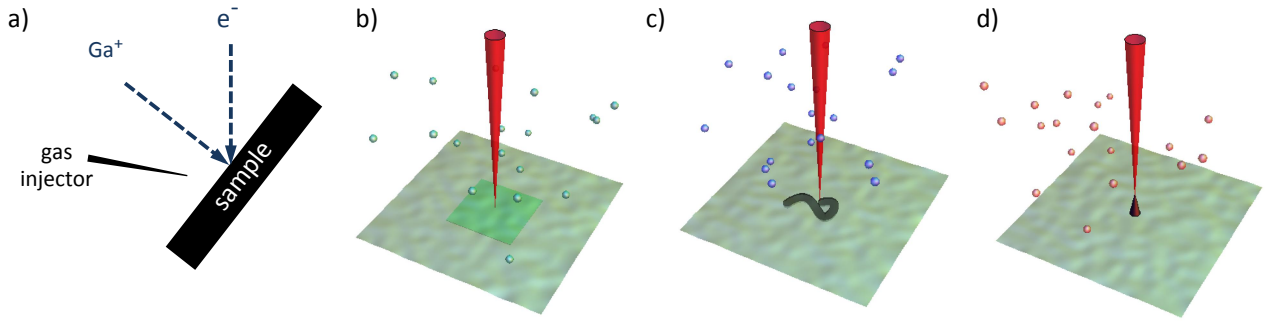

Figure 1: Schematic illustrations of: an electron-ion, dual beam system (a), and gas-mediated beam induced surface functionalization (b), chemical dry etching etching (c), and chemical vapor deposition (d).

The key distinguishing feature of this fabrication approach is that the beams can be used for imaging and iterative editing of nanostructures even if the substrate contains non-planar or inclined surfaces. The direct-write nature of the method is particularly attractive for multi-step process workflows as it overcomes alignment and feature placement problems inherent to mask-based lithographic methods. In the case of electron beam processing, spatial resolution better than 1 nm,

Laser 3D Manufacturing, edited by Henry Helvajian, Alberto Piqué, Martin Wegener, Bo Gu, Proc. of SPIE Vol. 8970, 89700O · © 2014 SPIE · CCC code: 0277-786X/14/$18 · doi: 10.1117/12.2042021

and 10 nm has been demonstrated using electron-transparent substrates [2] and bulk, electrical insulators {Toth:2007ac}, respectively (resolution is governed by the beam diameter, the area from which electrons are emitted from the substrate, charging and precursor molecule mass transport effects [1]).

Despite their versatility, wide deployment of these techniques has been limited by two problems in particular: (i) the serial nature of the methods translates to low throughput, which makes scalability challenging, and (ii) the fabricated structures often contain high concentrations of defects (particularly in the case of ion beam induced processing) and impurities (particularly in the case of electron beam induced deposition). Problems associated with scalability may eventually be overcome by exploiting novel bottom-up structure formation mechanisms such as that reported recently by Botman *et al.* [16]. Defects and impurities can be minimized by the use of electron (rather than ion) beams or post-growth processing techniques designed to yield high quality materials. Here we show how the quality of materials grown by electron beam induced deposition can be improved by: (i) post-growth annealing in a reactive, chemical ambient [17], and (ii) by the use of precursor molecules that undergo thermally activated transitions between multiple adsorption states on a growing surface [18,19]1. These process methodologies preserve the desired nanoscale size and shape of the deposits while enabling purities equivalent to those achieved by conventional deposition techniques such as chemical vapor deposition. We also demonstrate the fabrication of self-supporting, three dimensional nanostructures by electron beam induced chemical dry etching of single crystal diamond [20]. Significantly, the structures are luminescent, showing that the electron beam process does not degrade the optoelectronic properties of diamond.

2. REALIZATION OF HIGH PURITY MATERIALS GROWN BY ELECTRON BEAM INDUCED DEPOSITION

2.1 Post-growth purification

Most of the precursors used for electron beam induced deposition (EBID) are organometallics, as is the case in standard chemical vapor deposition. However, suitable EBID precursors must have both sufficiently high vapor pressures at or near room temperature, and high sticking coefficients and adsorption energies. In addition, because the fragments produced by electron dissociation often remain adsorbed on the sample surface for relatively long times, optimal deposition precursors should have a low content of carbon and other impurities in order to minimize incorporation of these species in the fabricated deposits.

These requirements limit the range of EBID precursors for high purity material deposition to a handful of compounds. Commonly used EBID precursors for metal deposition include methylcyclopentadienyl trimethyl platinum ($MeCpPtMe_3$) and tetrakis(trifluorophosphine) platinum ($Pt(PF_3)_4$) for Pt deposition [21,22]; dicobalt octacarbonyl ($Co_2(CO)_8$) for Co [3], and $W(CO)_6$ for tungsten [1]. However, materials grown by such precursors at room temperature typically contain high concentrations (5 to 90 at. %) of impurities [23]. We have recently realized high purity deposits using either elevated growth temperatures that enable thermally activated chemisorption of the precursor molecule [18], or post-growth annealing in a reactive gas such as water vapor [17].

We first discuss post-growth purification of Pt grown using $Pt(PF_3)_4$ as the deposition precursor gas. Pure platinum nanostructures are of interest for applications as interconnects in nano-electronics, nanodots for non-volatile memory, biosensors and fuel cells. In addition, Pt has very high activity for a wide range of nanoscale catalytic processes which enhance the performance of the material for solar energy conversion and proton exchange membrane fuel cells.

Although pure platinum deposits can be obtained from the metalorganic precursor $MeCpPtMe_3$ using a combination of a EBID-fabricated seed layer and atomic layer deposition (ALD) [24], this technique is extremely slow and cannot be used for controlled fabrication of high aspect ratio or nanoscale platinum because the deposits broaden laterally during ALD. A multi-step purification process has also been reported, whereby large area Pt films are deposited sequentially and purified by a combined oxygen irradiation and low temperature annealing process. However, this approach yields inhomogeneous deposit composition and nanostructure [21].

We performed Pt EBID using an environmental scanning electron microscope (ESEM) equipped with an environmental sub-chamber, previously described elsewhere [18,25]. Large deposits (approximately 5 μm diameter) suitable for compositional analysis by wavelength dispersive x-ray spectroscopy (WDS) were fabricated using a stationary, top-hat

electron beam. Nanoscale dot and pillar arrays were also fabricated by using a focused Gaussian electron beam of diameter approximately 1 nm (Fig. 2a and 2b).

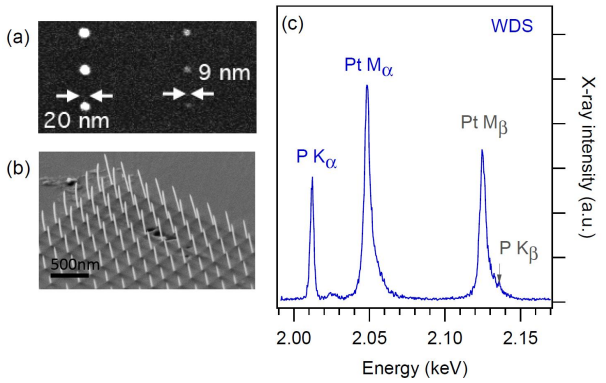

Figure 2. Electron micrographs of a Pt nanodot array (a), and an array of Pt nanopillars (b) grown by $Pt(PF_3)_4$ - mediated electron beam induced deposition. Both arrays were grown at room temperature using a 20keV, 0.2 nA, focused electron beam with a diameter of approximately 1 nm in ~0.1 Torr of $Pt(PF_3)_4$. Also shown is an X-ray spectrum showing the Pt K_α, Pt M_α, Pt M_β, P K_α, and K_β X-ray lines (c). [Adapted from [17].]

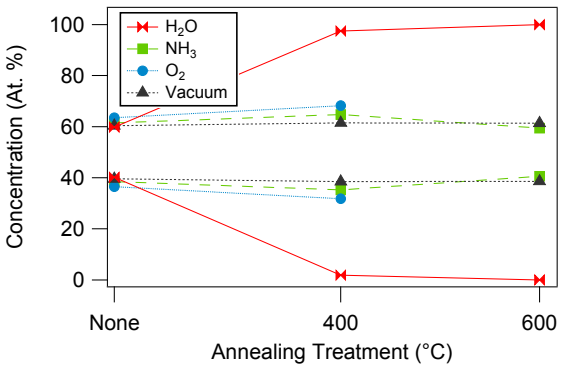

Figure 3. Purity of deposits grown by $Pt(PF_3)_4$-mediated electron beam induced deposition, before and after annealing treatments in water (H_2O), ammonia (NH_3), oxygen (O_2) and vacuum. [Adapted from [17].]

Deposits grown at room temperature have a typical atomic composition of 47 ± 5% Pt, 30 ± 5% P and 15 ± 10% O. The trace amounts of fluorine and the presence of oxygen in the as-grown deposits indicate efficient dissociation and desorption of PF_3 and fluorine during EBID, accompanied by oxidation of phosphorus by residual contaminants (mainly H_2O) present in the vacuum chamber. In order to remove the contaminants in the as-grown deposits, low temperature annealing was performed for 40 to 60 minutes per deposit in vacuum, and in H_2O, O_2 and NH_3 environments (pressure □ 130 Pa).

Annealing in vacuum, O_2 and NH_3 environments had no significant effect on composition at temperatures lower than the deposit decomposition temperature. However, low temperature (400-600° C) annealing in H_2O vapor can increase the Pt content to the point where it is indistinguishable from reference, high purity Pt films by WDS analysis (Fig. 3). The purification process is attributed to two mechanisms: mass transport of the (phosphorus) impurities to the deposit-H_2O interface followed by H_2O decomposition (and phosphorous volatilization) at the surface [17]. The mass transport process is the rate-limiting step and governs the purification rate. This study indicates that variations in the initial composition caused by deposition parameters such as the beam current density, the moisture content of the vacuum chamber used for EBID, and post-growth air exposure time do not affect the extent of purification. Hence, the purification method is likely extendable to other materials fabricated by EBID.

2.2 Purification by thermally activated chemisorption

Next, we describe a method that yields highly pure as-grown deposits, instead of requiring post-growth purification [18,19]. Electron beam induced deposition is typically done at or near room temperature using physisorbed precursor molecules [1]. In this scenario, thermal desorption causes a decrease in the deposition rate with increasing substrate temperature due to a corresponding decrease in precursor surface coverage (e.g. the blue trace in Fig. 4(a)). However, if the precursor can undergo activated chemisorption, and the chemisorption barrier is high relative to the thermal energy of the precursor gas and that of the substrate, then the deposition rate exhibits an increase with substrate temperature. This increase is caused by thermal transitions of adsorbates from the physisorbed to the chemisorbed state, and is followed by

a decrease caused by thermal desorption from the chemisorbed state (e.g. red trace in Fig. 4(a)). Adsorption kinetics associated with physisorption and activated chemisorption can be described using reaction coordinate diagrams such as the one shown in Fig. 4(b), where the reaction coordinate is the distance (z) above the sample surface, and the physisorbed and chemisorbed states are represented by potential wells separated by a chemisorption barrier of height E_C.

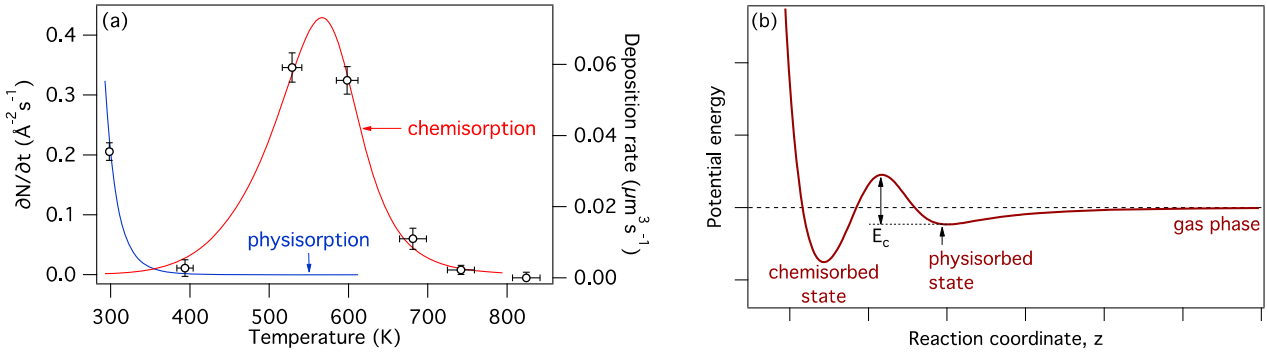

Figure 4. TEOS-mediated electron beam induced deposition of silicon oxide: temperature dependence of the measured deposition rate (points) and the corresponding calculated dissociation rates of physisorbed and chemisorbed precursor molecules (b). Also shown is a reaction coordinate diagram used to explain the observed dependence on substrate temperature (b). [Adapted from [18].]

Molecules such as $Si(OC_2H_5)_4$ (tetraethoxysilane, TEOS), a precursor for EBID of silicon oxide, can undergo both physisorption and activated chemisorption on a range of surfaces. Since deposition can be mediated by both physisorbed and chemisorbed species, the net deposition rate has a temperature dependence given by the sum of the physisorption and chemisorption components (e.g. the experimental data shown in Fig. 4(a)). Chemisorption therefore serves to enable EBID at elevated substrate temperatures which is desirable because it yields highly pure deposits. For example, in the case of the experimental data shown in Fig. 4(a), deposits grown below and above ~400 K contained significant and negligible amounts of carbon, respectively (the C content was quantified by energy dispersive x-ray spectroscopy which showed that the carbon-to-oxygen K_α x-ray peak ratio was ~ 0.25 and ~0.05 in deposits grown using physisorbed and chemisorbed adsorbates). The purity enhancement is ascribed to partial decomposition of the precursor molecules upon chemisorption, and efficient thermal desorption of carbon-containing fragments generated by electron induced dissociation of the adsorbates [18].

3. FABRICATION OF LUMINESCENT DIAMOND NANOSTRUCTURES

Color centers in diamond are promising candidates for photonic applications [26]. However, due to its inherent chemical and physical hardness, nanofabrication of diamond is challenging. Structuring optical cavities using reactive ion etching or ion beam techniques often involves residual damage and redeposition, which hinder device quality. Moreover, as diamond cannot be grown epitaxially on any other etchable substrate, producing thin, optically isolated diamond membranes is challenging. We have recently shown that electron beam induced etching (EBIE) can be used to fabricate suspended diamond structures through a chemical dry etch process that avoids redeposition and yields optically active nanostructures that are appropriate for photonic devices [20].

Scanning electron microscopes are a versatile fabrication tool with stages capable of high degrees of tilt and stability, and complex pattern generators that precisely steer the electron beam to desired positions through manipulation of the scan coils. By utilizing this advanced patterning and stage functionality, three dimensional nanostructures can be fabricated through EBIE. Modifications can be made to existing devices for defect repair, direct fabrication of material for rapid prototyping, or simple lamellas of material removed for further analysis.

The EBIE process utilizes low energy electrons, which do not cause damage through knock-on displacement of carbon, sputtering, and staining characteristic of reactive ion etching and focused ion beam sputtering techniques. Two variants of this process were demonstrated using single crystal diamond [20]. In the first, an etch mask was used to define the geometry of high aspect ratio nanostructures. In the second, mask-free direct-write EBIE [15,27-29] was used to pattern

microdiamonds. Here, a suspended one dimensional bridge structure that is commonly used in photonic and optomechanical applications was fabricated by direct-write EBIE (Fig. 5).

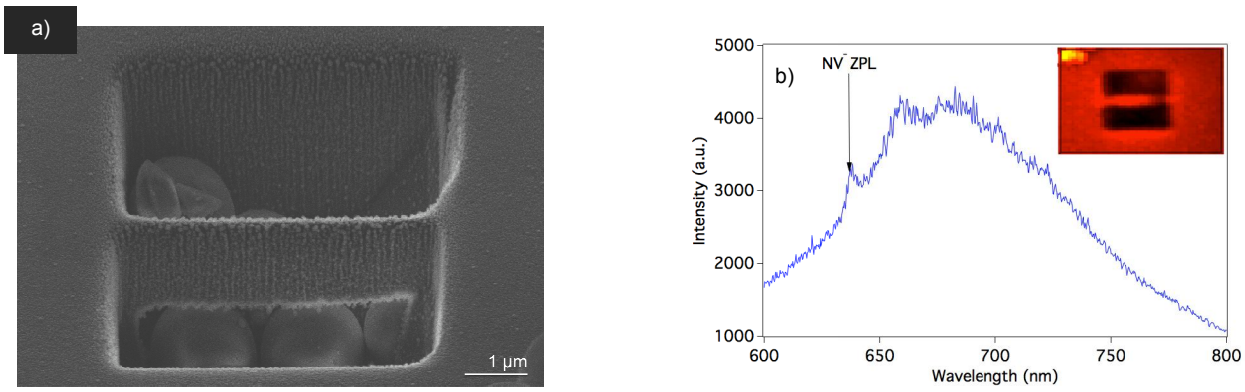

Figure 5 (a) SEM image (stage tilt = 45°) of a bridge structure fabricated in CVD grown single crystal diamond (100 face) by direct-write H_2O-mediated EBIE using a 2 keV electron beam and a H_2O pressure of 13 Pa. The bridge is 600 nm wide and 6.5 μ m long. The depth of the undercut is indicated by 2 μ m silica beads. (b) Photoluminescence spectra measured from the diamond bridge structure, showing emission from the nitrogen-vacancy (NV) color center. *Inset:* Photoluminescence intensity scan of bridge and surrounding diamond. [Adapted from Martin:2013ue.]

The free standing bridge structure shown in Fig. 5(a) was produced by etching two adjacent 5 μ m deep boxes using H_2O mediated EBIE. After etching, the SEM stage was tilted to 35° and the side of the bridge further etched at this angle to produce the undercut. The bridge geometry and dimensions, including the width, length, gap height and cutting angle can all be adjusted using the electron beam and SEM stage parameters. Photoluminescence (PL) (Fig. 5(b)) and Raman analyses [20] of the fabricated structure reveal that the unique optical properties of diamond are maintained and no graphitization occurs.

This powerful addition to the toolkit for diamond nanofabrication enables *in situ* mask-less etching with nanoscale resolution without the need for ion sputtering or mask-based lithography. The technique enables the fabrication of free-standing structures in diamond free from defects, damage and surface contamination caused by the charged particle irradiation.

4. SUMMARY

Charged particle beam chemical processing techniques enable direct-write fabrication and iterative editing of nanostructured materials. Electron beam processing is particularly attractive because of low defect generation rates and the absence of staining characteristic of analogous ion beam processing methods. Here we demonstrated the fabrication of luminescent, single-crystal diamond nanostructures by electron beam induced etching, and two approaches for the deposition of high purity materials by electron beam induced deposition. The latter entail the use of precursor molecules that undergo chemisorption at elevated substrate temperatures, and a post-growth, thermally-activated chemical purification technique.

REFERENCES

[1] I. Utke, S. Moshkalev, and P. Russell, *Nanofabrication Using Focused Ion and Electron Beams*, Oxford University Press, USA (2012).

[2] W. F. van Dorp, B. Van Someren, C. W. Hagen, and P. Kruit, "Approaching the resolution limit of nanometer-scale electron beam-induced deposition," *Nano Lett.* **5**(7), 1303–1307 (2005).
[3] A. Fernández-Pacheco, L. Serrano-Ramón, J. M. Michalik, M. R. Ibarra, J. M. De Teresa, L. O'Brien, D. Petit, J. Lee, and R. P. Cowburn, "Three dimensional magnetic nanowires grown by focused electron-beam induced deposition," *Sci. Rep.* **3**, 1492 (2013).
[4] I. Utke, P. Hoffmann, R. Berger, and L. Scandella, "High-resolution magnetic Co supertips grown by a focused electron beam," *Appl. Phys. Lett.* **80**(25), 4792–4794 (2002).
[5] V. Gopal, V. R. Radmilovic, C. Daraio, S. Jin, P. D. Yang, and E. A. Stach, "Rapid prototyping of site-specific nanocontacts by electron and ion beam assisted direct-write nanolithography," *Nano Lett.* **4**(11), 2059–2063 (2004).
[6] K. Hoeflich, R. B. Yang, A. Berger, G. Leuchs, and S. Christiansen, "The Direct Writing of Plasmonic Gold Nanostructures by Electron-Beam-Induced Deposition," *Adv. Mater.* **23**(22-23), 2657–2661 (2011).
[7] M. G. Jenke, D. Lerose, C. Niederberger, J. Michler, S. Christiansen, and I. Utke, "Toward Local Growth of Individual Nanowires on Three-Dimensional Microstructures by Using a Minimally Invasive Catalyst Templating Method," *Nano Lett.* **11**(10), 4213–4217 (2011).
[8] T. Lukasczyk, M. Schirmer, H. P. Steinruck, and H. Marbach, "Generation of Clean Iron Structures by Electron-Beam-Induced Deposition and Selective Catalytic Decomposition of Iron Pentacarbonyl on Rh(110)," *Langmuir* **25**(19), 11930–11939 (2009).
[9] M. Walz, M. Schirmer, F. Vollnhals, T. Lukasczyk, H. P. Steinruck, and H. Marbach, "Electrons as 'Invisible Ink': Fabrication of Nanostructures by Local Electron Beam Induced Activation of SiOx," *Angew Chem Int Edit* **49**, 4669–4673 (2010).
[10] F. Vollnhals, P. Wintrich, M. M. Walz, H. P. Steinruck, and H. Marbach, "Electron Beam Induced Surface Activation of Ultrathin Porphyrin Layers on Ag(111)," *Langmuir* **29**(39), 12290–12297 (2013).
[11] F. Vollnhals, T. Woolcot, M. M. Walz, S. Seiler, H. P. Steinruck, G. Thornton, and H. Marbach, "Electron Beam-Induced Writing of Nanoscale Iron Wires on a Functional Metal Oxide," *The Journal of Physical Chemistry C* **117**(34), 17674–17679 (2013).
[12] K. Muthukumar, H. O. Jeschke, R. Valentí, E. Begun, J. Schwenk, F. Porrati, and M. Huth, "Spontaneous dissociation of $Co_2(CO)_8$ and autocatalytic growth of Co on SiO_2: A combined experimental and theoretical investigation," *Beilstein J. Nanotechnol.* **3**, 546–555 (2012).
[13] S. J. Randolph, A. Botman, and M. Toth, "Deposition of Highly Porous Nanocrystalline Platinum on Functionalized Substrates Through Fluorine-Induced Decomposition of $Pt(PF_3)_4$ Adsorbates," *Particle* **30**(8), 672–677 (2013).
[14] M. N. Khan, V. Tjong, A. Chilkoti, and M. Zharnikov, "Fabrication of ssDNA/Oligo(ethylene glycol) Monolayers and Complex Nanostructures by an Irradiation-Promoted Exchange Reaction," *Angew Chem Int Edit* **51**(41), 10303–10306 (2012).
[15] A. A. Martin, M. R. Phillips, and M. Toth, "Dynamic Surface Site Activation: A Rate Limiting Process in Electron Beam Induced Etching," *ACS Appl. Mater. Interfaces* **5**(16), 8002–8007 (2013).
[16] A. Botman, A. Bahm, S. Randolph, M. Straw, and M. Toth, "Spontaneous Growth of Gallium-Filled Microcapillaries on Ion-Bombarded GaN," *Phys. Rev. Lett.* **111**(13), 135503 (2013).
[17] C. Elbadawi, M. Toth, and C. J. Lobo, "Pure Platinum Nanostructures Grown by Electron Beam Induced Deposition," *ACS Appl. Mater. Interfaces* **5**, 9372–9376 (2013).
[18] J. Bishop, C. J. Lobo, A. Martin, M. Ford, M. R. Phillips, and M. Toth, "The role of activated chemisorption in electron beam induced deposition," *Phys. Rev. Lett.* **109**, 146103 (2012).
[19] J. Bishop, M. Toth, M. Phillips, and C. Lobo, "Effects of oxygen on electron beam induced deposition of SiO_2 using physisorbed and chemisorbed tetraethoxysilane," *Appl. Phys. Lett.* **101**(21), 211605 (2012).
[20] A. Martin, M. Toth, and I. Aharonovich, "Subtractive 3D Printing of Diamond," *submitted* (2014).
[21] S. Mehendale, J. J. L. Mulders, and P. H. F. Trompenaars, "A new sequential EBID process for the creation of pure Pt structures from MeCpPtMe3," *Nanotechnology* **24**(14), 145303 (2013).
[22] J. D. Barry, M. Ervin, J. Molstad, A. Wickenden, T. Brintlinger, P. Hoffman, and J. Meingailis, "Electron beam induced deposition of low resistivity platinum from $Pt(PF_3)_4$," *J. Vac. Sci. Technol. B* **24**(6), 3165–3168 (2006).
[23] A. Botman, J. J. L. Mulders, and C. W. Hagen, "Creating pure nanostructures from electron-beam-induced deposition using purification techniques: a technology perspective," *Nanotechnology* **20**(37), 372001 (2009).
[24] A. J. M. Mackus, J. J. L. Mulders, M. C. M. van de Sanden, and W. M. M. Kessels, "Local deposition of high-

purity Pt nanostructures by combining electron beam induced deposition and atomic layer deposition," *J. Appl. Phys.* **107**(11), 116102 (2010).
[25] C. J. Lobo, A. Martin, M. R. Phillips, and M. Toth, "Electron beam induced chemical dry etching and imaging in gaseous NH_3 environments," *Nanotechnology* **23**(37), 375302 (2012).
[26] C. J. H. Wort and R. S. Balmer, "Diamond as an electronic material," *Mater Today* **11**(1-2), 22–28 (2008).
[27] J. Taniguchi, I. Miyamoto, N. Ohno, and S. Honda, "Electron beam assisted chemical etching of single crystal diamond substrates," Japanese Journal of Applied Physics Part 1, 1996, 6574–6578.
[28] J. Taniguchi, I. Miyamoto, N. Ohno, K. Kantani, M. Komuro, and H. Hiroshima, "Electron beam assisted chemical etching of single-crystal diamond substrates with hydrogen gas," Japanese Journal of Applied Physics Part 1, 1997, 7691–7695.
[29] J.-I. Niitsuma, X.-L. Yuan, S. Koizumi, and T. Sekiguchi, "Nanoprocessing of Diamond Using a Variable Pressure Scanning Electron Microscope," *Jpn. J. Appl. Phys.* **45**(No. 2), L71–L73 (2006).